EurJIC
European Journal of Inorganic Chemistry

Full Papers
doi.org/10.1002/ejic.202000879

Chemistry Europe
European Chemical Societies Publishing

Platinum(II) Complexes of Tridentate $N^{\wedge}N^{-}{}^{\wedge}N$ -Coordinating Ligands Based on Imides, Amides, and Hydrazides: Synthesis and Luminescence Properties

Emma V. Puttock,[a] Jiri Sturala,[b] Jos C. M. Kistemaker,[c] and J. A. Gareth Williams*[a]

Five Pt(II) complexes are described in which the metal ion is bound to anionic $N^{\wedge}N^{\wedge}N$-coordinating ligands. The central, deprotonated N atom is derived from an imide Ar–C(=O)–NH–C(=O)–Ar {$PtL^{1-2}Cl$; Ar = pyridine or pyrimidine}, an amide py–C(=O)–NH–CH_2–py {PtL^3Cl}, or a hydrazide py–C(=O)–NH–N=CH–py {PtL^4Cl}. The imide complexes $PtL^{1-2}Cl$ show no significant emission in solution but are modestly bright green/yellow phosphors in the solid state. PtL^3Cl is weakly phosphorescent. PtL^4Cl is formed as a mixture of isomers, bound through either the amido or imino nitrogen, the latter converting to the former upon absorption of light. Remarkably, the imino form displays fluorescence in solution, $\lambda^{0,0} = 535$ nm, whereas the amido shows phosphorescence, $\lambda^{0,0} = 624$ nm, $\tau = 440$ ns. It is highly unusual for two isomeric compounds to display emission from states of different spin multiplicity. The amido-bound PtL^4Cl can act as a bidentate $O^{\wedge}N$-coordinating ligand, demonstrated by the formation of bimetallic complexes with iridium(III) or ruthenium(II).

Introduction

Metal complexes of pincer ligands occupy a prominent position in modern organometallic chemistry.[1] The term 'pincer' is used to describe monoanionic tridentate ligand platforms that feature a central anionic site bound to the metal, flanked by two charge-neutral ligating units such as amines, imines, pyridines, phosphines or sulfides. In many instances, the central anionic unit is formally a deprotonated benzene ring – *i.e.*, a cyclometallated aromatic unit – giving $E^{\wedge}C^{\wedge}E$ coordination (*e.g.*, *E* = N, P, S). The strongly σ-donating cyclometallated ring in combination with, for example, lateral π-accepting pyridines (Figure 1a) leads to strong ligand fields.[2] Thus, in the resulting complexes with d^8 metal ions such as Ni(II), Pd(II), Pt(II), Ir(I) and Au(III), a square-planar coordination geometry typically arises, with the fourth site occupied by a relatively weakly bound monodentate ligand *X*, such as a halide. The robustness of the M(*ECE*) unit, coupled with the lability of the M–*X* bond for some metals like Ni(II) and Pd(II), underpins much of the success of pincer complexes in homogeneous catalysis.[3]

In the field of inorganic photochemistry and photophysics, square-planar platinum(II) complexes continue to offer much interest to researchers.[4] The high spin-orbit coupling constant of Pt can greatly facilitate formally forbidden triplet phosphorescence in complexes with aromatic ligands.[5] Over the past 15 years, a number of very brightly phosphorescent complexes of Pt(II) have been reported.[4] Some have opened up new avenues of research in bio-imaging[6] and sensing[7] whilst others have attracted interest as potential phosphors for OLEDs.[8] Unlike related complexes of d^6 metal ions such as Ir(III), the propensity of these flat Pt(II) molecules to undergo face-to-face interactions can lead to the generation of excimers and/or aggregates that may emit at lower energy, leading to further scope in accessing deep red/NIR emitters and/or generation of white light using a single OLED dopant.[9]

Key to the design of luminescent platinum(II) complexes is to build into the molecule a high degree of rigidity, in order to ensure that potentially competitive non-radiative decay pathways are minimised.[10] Certain pincer-type complexes of Pt(II) offer such rigidity and are luminescent under ambient conditions. For example, Pt(II) complexes of 1,3-di(2-pyridyl) benzene (dpybH) and its derivatives, such as Pt(dpyb)Cl (Figure 1b), are intensely luminescent in solution at room temperature.[11] They are readily amenable to colour tuning and form strongly emissive excimers: they have shown promise as OLED emitters in the visible and NIR,[12] and as long-lived probes for bioimaging.[13] Despite this promise, there are some drawbacks to systems based on such $N^{\wedge}C^{\wedge}N$-coordinating ligands. These ligands are synthesised most readily from palladium-catalysed cross-coupling reactions.[14] They require use of relatively costly precursors – either pyridyl stannanes (which are toxic) in the case of Stille reactions or benzene diboronic acids

[a] *Dr. E. V. Puttock, Prof. Dr. J. A. G. Williams*
Department of Chemistry
Durham University
DH1 3LE, U.K. Durham
E-mail: j.a.g.williams@durham.ac.uk
www.dur.ac.uk/chemistry/staff/profile/?id = 205
[b] *Dr. J. Sturala*
Department of Inorganic Chemistry
University of Chemistry and Technology Prague
Technicka 5, 166 28 Prague 6, Czech Republic
[c] *Dr. J. C. M. Kistemaker*
Centre for Organic Photonics and Electronics, The School of Chemistry and Molecular Biosciences
University of Queensland
4072 Queensland, Australia

Supporting information for this article is available on the WWW under https://doi.org/10.1002/ejic.202000879

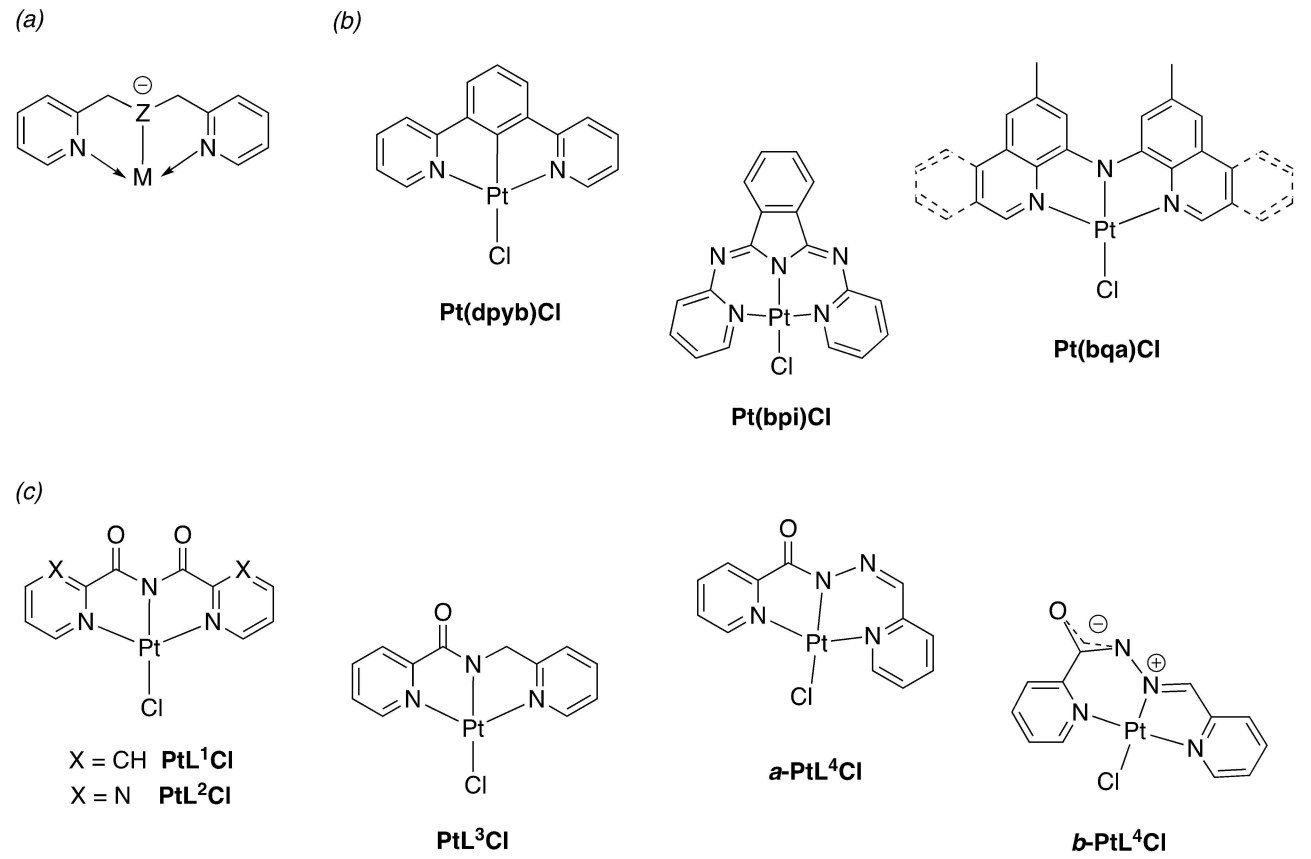

Figure 1. (a) Generic structure of a metal coordinated to a pincer ligand featuring flanking pyridyl rings, where Z is typically a carbon or nitrogen atom. (b) Previous examples of related pincer Pt(II) complexes: Pt(dpyb)Cl (i.e., Z=C); Pt(bpi)Cl and Pt(bqa)Cl (Z=N). Phenanthridinyl analogues of Pt(bqa)Cl are represented by the dashed lines. (c) Structures of the complexes PtL^1Cl–PtL^4Cl investigated in this work.

in the case of the alternative Suzuki strategy. Their reliance on Pd catalysts can also lead to trace palladium contamination in final products, undesirable in the photonic industry.

We, and others, have been interested in using deprotonated azole units in place of cyclometallated rings; *i.e.*, N^- donors in place of C^-.[15,16] For example, 2-pyridylbenzimidazole proves to be an attractive alternative to phenylpyridine in bidentate Ir(III) complexes,[15a] whilst Chi and co-workers have pioneered the use of a variety of bidentate ligands incorporating triazoles that bind through deprotonation.[16] Nevertheless, few pincer complexes of Pt(II) with a central anionic nitrogen have been investigated for luminescence. The most notable examples are Pt(bpi)Cl and a limited number of its derivatives {bpi = 1,3-bis(2-pyridylimino)isoindoline, Figure 1b}, and very recent work on bis(8-quinolyl)amine and bis(4-phenanthridinyl)amine complexes {*e.g.* Pt(bqa)Cl, Figure 1b}. They show weak, deep-red luminescence under ambient conditions.[17,18,19]

In this contribution, we have sought to examine Pt(II) complexes of other pincer ligands of the type N^{het}–N^-–N^{het} (N^{het} = an N-heterocycle such as pyridine), aiming to identify whether they may offer scope in providing access to new phosphorescent molecular materials. We describe the synthesis of four such ligands and their Pt(II) complexes, together with their luminescence properties. Analogous Pd(II) complexes have previously been reported. One of the complexes has the potential to bind a second metal ion as an *N^O*-bidentate ligand, as evidenced by the formation of two heterometallic dinuclear compounds with Ru(II) and Ir(III) units.

Results and Discussion

Synthesis

The target mononuclear complexes are shown in Figure 1c. PtL^1Cl and PtL^3Cl have been isolated previously by others, the latter inadvertently as an unexpected product involving quite different chemistry.[20] The synthetic pathways to the requisite ligands and their complexes are summarised in Scheme 1.

The ligand HL^1, known as bis(2-pyridylcarbonyl)amide or bca, has been studied for many years in the context of metal complexes for single-molecule magnets, catalysis of CO_2 reduction, and coordination polymers.[21,22] It was originally obtained as an unexpected product of metal-catalysed hydrolysis of 2,4,6-tris(2-pyridyl)-1,3,5-triazine (tpyt).[21] That reaction lends itself well to the synthesis of gram quantities of the ligand; the procedure was employed here using copper nitrate followed by treatment with EDTA to remove the metal

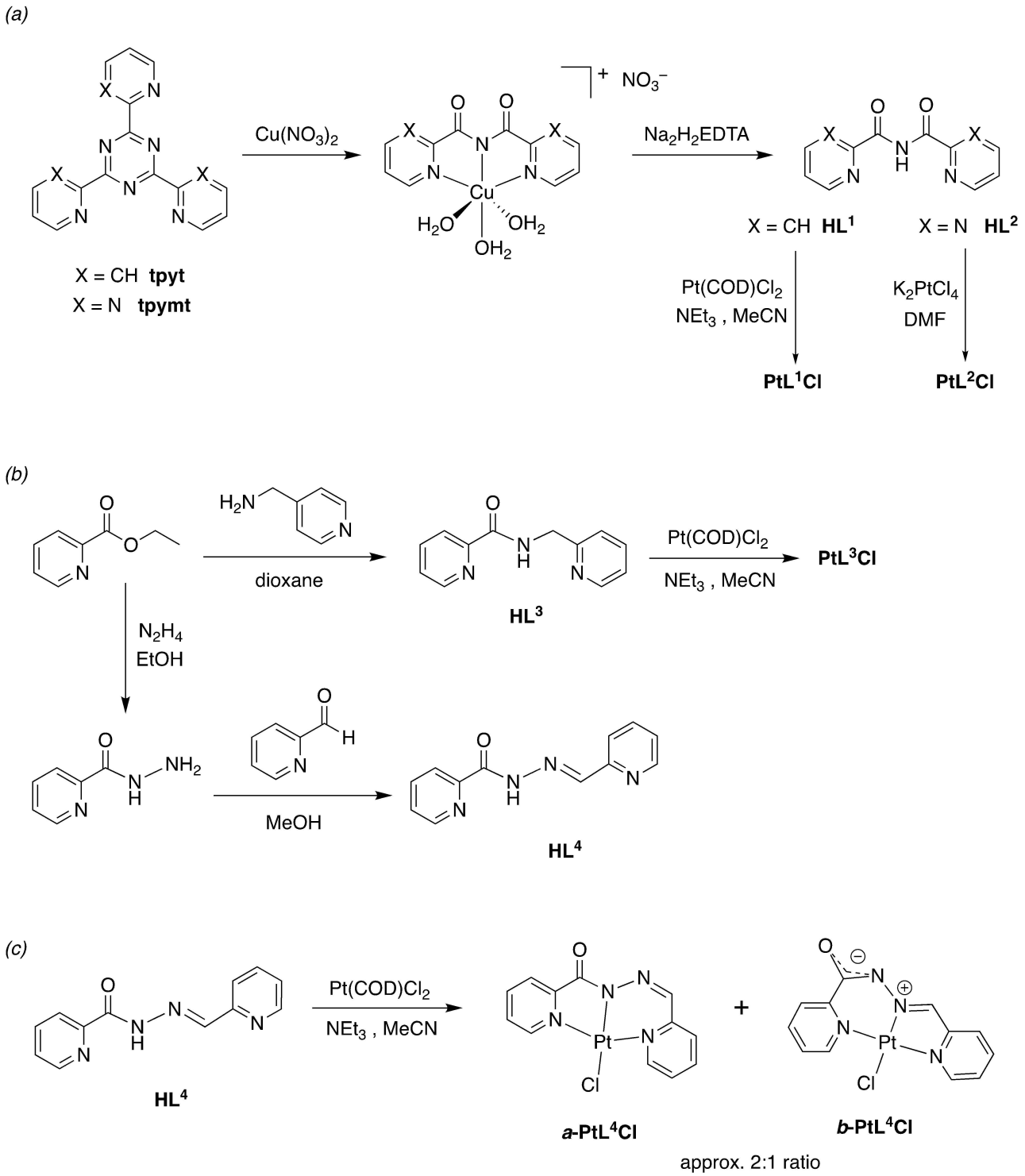

Scheme 1. Synthesis of the proligands and their corresponding Pt(II) complexes.

(Scheme 1a). A similar procedure allows access to HL^2 from 2,4,6-tris(2-pyrimidyl)-1,3,5-triazine (tpymt). The precursor tpymt was obtained by cyclotrimerisation of 2-cyanopyrimidine at 150 °C. Contrary to previous reports in which arduous purification was required,[21] we found that this reaction gave tpymt in 80% yield, in sufficient purity for subsequent use, by using a simple ether wash. Ligand HL^3, *N*-(2-picolyl)-picolinamide, is accessible in one simple step to form the amide bond, by reaction of ethyl 2-picolinate with 2-picolylamine under microwave irradiation for 1 h (Scheme 1b).[23] Meanwhile, HL^4 – an acylhydrazone or hydrazide – was prepared in two steps by the initial formation of 2-picolylhydrazine from ethyl 2-picolinate

and hydrazine, followed by condensation with pyridyl-2-carboxaldehyde to form the imine bond and thus introduce the second pyridine ring (Scheme 1b). As previously discussed by Hecht and co-workers for a range of other acylhydrazones, we observed exclusive formation of the *E*-isomer of HL^4 by ^{1}H NMR spectroscopy, with no evidence of the *Z* form being present.[24] Clearly, if HL^4 is to coordinate in a tridentate fashion to a single metal ion, then isomerisation to the *Z* form will need to occur.

The complexes PtL^1Cl and PtL^3Cl were readily prepared by reaction of the respective ligands HL^1 and HL^3 with $Pt(COD)Cl_2$ in acetonitrile solution, in the presence of triethylamine as a base to facilitate deprotonation of the central N–H. They are both bright yellow solids. The same procedure did not lend itself well to the preparation of PtL^2Cl, owing to poor solubility. This complex was prepared instead by reaction of HL^2 with K_2PtCl_4 in DMF. The resulting complex was only poorly soluble, and it was separated from traces of residual ligand by crystallisation from hot DMSO, again giving yellow crystals.

The reaction of HL^4 with $Pt(COD)Cl_2$ in the presence of NEt_3 led to a dark purple solid, which was found by ^{1}H NMR to consist of a mixture of primarily two Pt(II) complexes. The two complexes could be successfully separated by column chromatography on silica. The first complex to elute is burnt orange in colour and is appreciably soluble in chlorinated solvents, whereas the second complex is dark purple, having more limited solubility. The two complexes have identical masses by mass spectrometry, both corresponding to the expected composition PtL^4Cl, suggesting that they are isomeric; they will be referred to henceforth as *a*-PtL^4Cl and *b*-PtL^4Cl respectively. We noted that, in solution, the *b* form gradually converted to the *a* form under ambient room lighting, as monitored by ^{1}H NMR spectroscopy.

Nakajima and co-workers have previously explored the coordination chemistry of the same ligand HL^4 with palladium.[25] They were able to isolate three products, depending on the conditions, each identified crystallographically: a complex of the form $Pd(N^\wedge N\text{-}HL^4)Cl_2$ featuring the non-deprotonated ligand HL^4 bound to the metal in an $N^\wedge N$ manner through the pyridylimine unit; and a pair of isomeric complexes of composition $Pd(N^\wedge NN\text{-}L^4)Cl$, featuring the deprotonated ligand bound in a tridentate fashion. These two isomers differ according to which is the central nitrogen atom: either the amido nitrogen (as in form *a* of PtL^4Cl in Scheme 1c) or the imino nitrogen (form *b*). The latter palladium complex converted to the former in solution in the presence of light, whilst $Pd(N^\wedge N^\wedge N\text{-}HL^4)Cl_2$ also converted to the tridentate amido form thermally, indicating that the amido form is the thermodynamically favoured product. We were not able to obtain crystals of the Pt(II) complexes of sufficient quality for structural confirmation by X-ray diffraction. However, the ^{1}H NMR spectra of our *a* and *b* Pt(II) isomers closely match those of the crystallographically confirmed amido and imino Pd(II) complexes respectively: the four spectra are reproduced collectively for comparison in Figure S1 in the Supporting Information. Based on these observations, together with the light-activated *b*→*a* conversion, there can be little doubt that the isomers *a*-PtL^4Cl and *b*-PtL^4Cl correspond to the amido and imino-bound forms respectively, as labelled in Scheme 1.

Further support for the assignment is provided by DFT calculations, which were carried out on the two Pt(II) isomers using one of three functionals (CAM-B3LYP, BMK, or ωB97X-D), with Def2-TZVP as the basis set and with the dichloromethane solvent taken into account using the conductor-like polarised continuum model (C-PCM). Details are given in the Experimental Section, and atomic coordinates of the optimised ground-state structures are listed in Section 5 of the Supporting Information. The calculations reveal that the imino *b*-PtL^4Cl isomer is unequivocally less stable than the amido *a*-PtL^4Cl by around 52 kJ mol^{-1} (values of 52.4, 51.4 and 52.8 kJ mol^{-1} were obtained using the three functionals listed above, respectively), consistent with the experimentally observed *b*→*a* interconversion.

Bimetallic complexes

Dipyridylcarbonyl complexes of 1st row transition metals have previously been used in the construction of multinuclear systems and coordination polymers: the deprotonated C(=O)–N–C(=O) unit resembles $acac^-$ (Hacac = 2,4-pentanedione, commonly known as acetylacetone) and may thus be able to bind to a metal in a bidentate $O^\wedge O$-chelating manner.[19] Given the recent interest in dinuclear Pt–Ir complexes,[26] coupled with the ubiquity of bis-cyclometallated iridium chemistry in the field of luminescence, we reasoned that it could be of interest to examine the PtL^1Cl unit as a bidentate ligand to iridium(III) in an $Ir(N^\wedge C)_2(L^\wedge L)$ complex. The standard iridium precursor $[Ir(ppy)_2(\mu\text{-}Cl)]_2$ was treated with PtL^1Cl (2 equiv.) under conditions typically used to prepare $[Ir(N^\wedge C)_2(O^\wedge O\text{-acac})]$ complexes, namely the use of a mixed DCM/MeOH solvent system at a temperature of 65 °C. However, there was no clear spectroscopic evidence for the formation of the desired product, even after prolonged reaction times. It may be noted that, although the biscarbonylamide ligand is deprotonated, the combination with Pt in oxidation state +2 and the monodentate chloride leads to a net charge on the PtL^1Cl unit of zero, as opposed to −1 on acac in Ir(III) complexes with acac as an $O^\wedge O$ ligand. The charge neutrality probably makes the PtL^1Cl unit a poor ligand for Ir(III). The known examples in which charge-neutral $M(bca)_2$ complexes act as ligands are in combination with "harder", more oxophilic metal ions such as Mn^{2+} and Fe^{3+}.[19]

The complex PtL^4Cl also has the potential to bind to a second metal ion, in this case as a charge-neutral $O^\wedge N$-chelating ligand. Indeed, Nakajima and co-workers previously prepared a dinuclear Pd–Ru complex starting from a ligand similar to L^4, but with a 2-quinolyl as opposed to 2-pyridyl pendant on the imine.[27] We found that treatment of *a*-PtL^4Cl with $[Ir(ppy)_2(\mu\text{-}Cl)]_2$ (2:1 ratio) in DCM/MeOH at 65 °C successfully gave the desired heterodinuclear complex $[PtCl(\mu\text{-}L^4)Ir(ppy)_2]PF_6$ as a dark green solid after anion exchange in aqueous KPF_6 (Scheme 2). To allow a direct comparison with the palladium work of Nakajima, *a*-PtL^4Cl was also treated with $RuCl_2(PPh_3)_2$ to form the charge-neutral Pt(II)–Ru(II) complex $[PtCl(\mu\text{-}L^4)RuCl_2(PPh_3)_2]$.

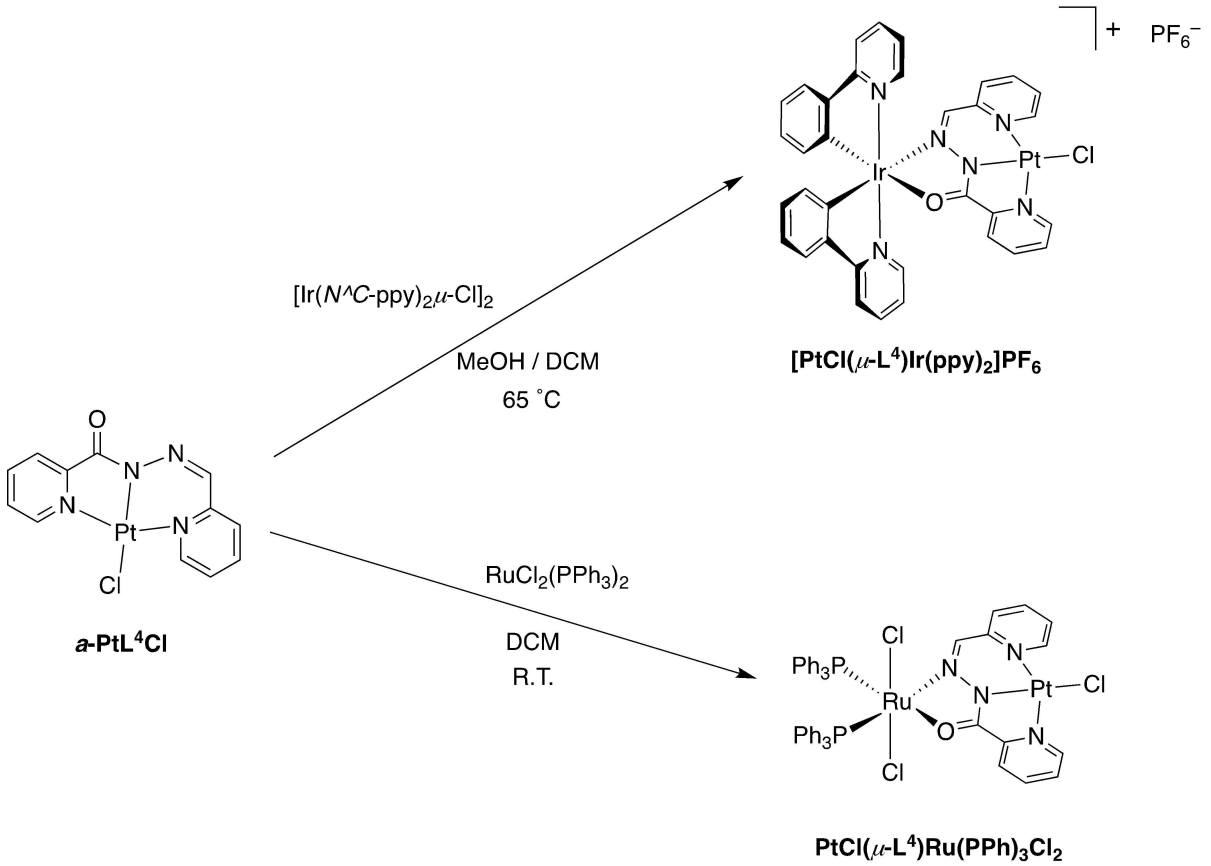

Scheme 2. Synthesis of the dimetallic compounds from the mononuclear Pt(II) complexes.

Complexation to Ru(II) was accompanied by a large up-field shift of the imine proton in the ^{1}H NMR spectrum, fully consistent with the Pd–Ru complex.[27] As potential ligands, both PtL^{4}Cl and PtL^{1}Cl are charge-neutral, rather than anionic. The fact that PtL^{4}Cl can successfully act as an *O^N* bidentate ligand to Ir(III), whereas there is no evidence of *O^O* binding of PtL^{1}Cl to Ir(III), may be a reflection of the "softer" character of iridium, favouring binding of more polarisable nitrogen donors over harder, exclusively oxygen donors.

Photophysical properties of the mononuclear complexes PtL$^{1-4}$Cl

(i) Absorption

The imide-based complexes PtL$^{1-3}$Cl are very poorly soluble in all common organic solvents. Their UV-visible absorption spectra in dilute dichloromethane solution at ambient temperature are shown in Figure 2 (numerical values are included amongst the characterisation data for each complex in the Experimental Section). The complexes show very strong absorption bands at $\lambda < 300$ nm, which may be attributed to π–π* transitions within the aromatic rings of the ligands: bands of comparable intensity are observed in the same region for the free ligands. The somewhat weaker bands at longer wavelengths have no counterpart in the free ligands and are thus likely to be due to charge-transfer (CT) transitions involving the metal. Based on the structural similarity of the complexes to Pt(dpyb)Cl and on the experimental and theoretical studies on such complexes,[11,12] the lowest-energy CT transitions are likely to involve charge-transfer from filled orbitals spanning the Pt centre, the chloride and probably also the central N atom, to π* orbitals based on the heterocycles. TD-DFT calculations on PtL^{1}Cl in the S_0 state confirm this expected localisation of the frontier orbitals (Figure S2 in the Supporting Information).

Such an interpretation readily accounts for the observed trend in energies amongst the three complexes PtL$^{1-3}$Cl. Thus, the red-shift in the lowest-energy absorption band on going from PtL^{1}Cl to PtL^{2}Cl will arise as a result of the lower-energy of π* orbitals on pyrimidine compared to pyridine rings. In PtL^{3}Cl (which lacks the C_{2v} symmetry of PtL$^{1-2}$Cl), the lowest-energy π* orbitals would be expected to be those based on the py–C=O (*i.e.*, as in PtL^{1}Cl) as opposed to the py–CH_2 ring, due to the electron-withdrawing nature of the carbonyl unit. The red-shift compared to PtL^{1}Cl, therefore, likely arises not from a significant difference in the LUMO energy but rather from the platinum-based HOMO being displaced to somewhat higher energies, owing to the Pt being coordinated by a more electron-rich py–CH_2 unit. The interpretation is supported by absorption

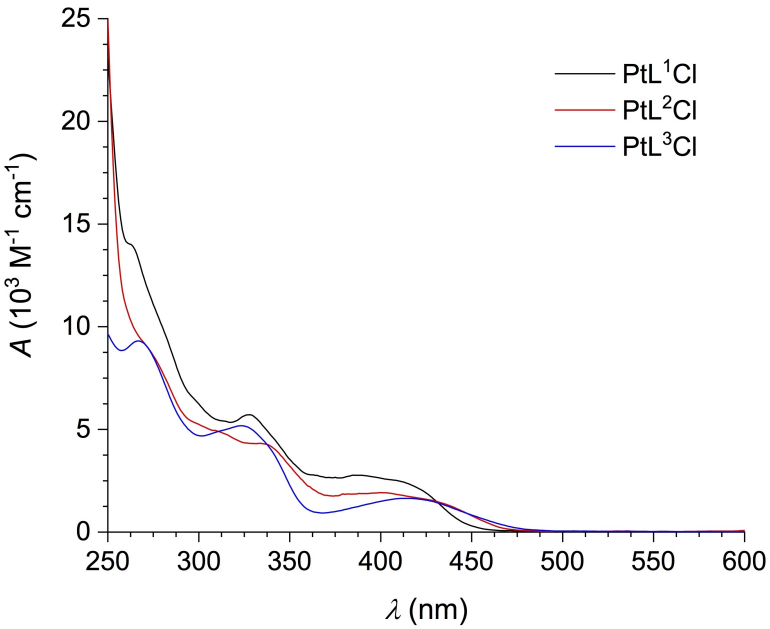

Figure 2. UV-Vis absorption spectra of $PtL^{1-3}Cl$ in CH_2Cl_2 at 295 ± 3 K.

spectra modelled using the lowest-energy series of excited states of the three complexes obtained by DFT using the aforementioned functionals. The simulated spectra show the same trend of decreasing energy of the first spin-allowed absorption band in the order $PtL^1Cl > PtL^2Cl > PtL^3Cl$ (Figures S5–S7 in the Supporting Information).

The absorption spectra of the two isolated forms of the hydrazide complex, *a/b*-PtL^4Cl, are shown in Figure 3. To the eye, these compounds are more strongly coloured than those of $PtL^{1-3}Cl$ and indeed the spectra of both forms reveal a more intense band further into the visible than the lowest-energy band of the other complexes, centred around 470 nm. Similarly intense and well-defined bands were observed by Nakajima and co-workers for palladium complexes *a/b*-PdL^4Cl, albeit at slightly shorter wavelength (450 nm), assigned to transitions of predominantly π–π* character within the hydrazide unit.[27] The transition must be influenced by the metal too, given that the change from Pd to Pt lowers the energy of the band by around 1000 cm^{-1}. The molar absorptivities of the *a* form are significantly lower than those of the *b* isomer across almost all wavelengths, and by a factor of about 2 for the longest wavelength λ_{max} values (Figure 3). The theoretical spectra

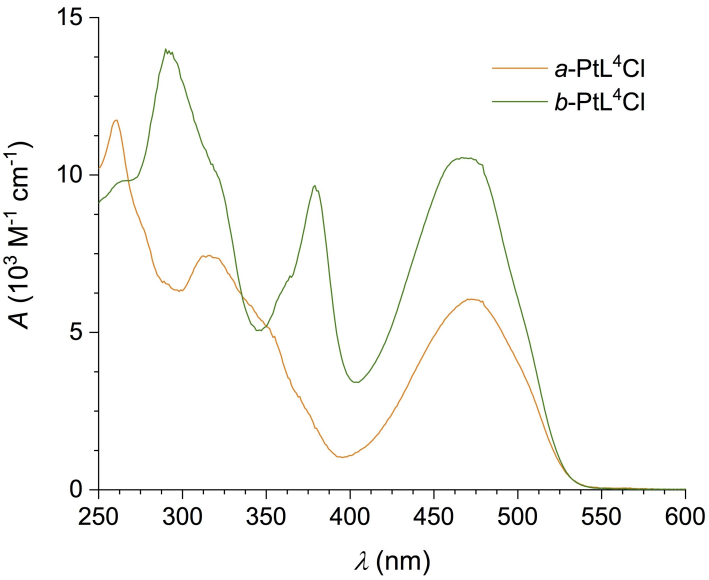

Figure 3. UV-Vis absorption spectra of the two isomers of PtL^4Cl in CH_2Cl_2 at 295 ± 3 K.

calculated with various DFT functionals closely match the experimental ones (Figures S8 and S9). Moreover, the higher molar aborptivity of the *b* isomer is consistent with the higher calculated oscillator strengths *f* of most of the transitions (*e.g.*, for the lowest-energy transition, $f = 0.25$ and 0.40 for the *a* and *b* isomers respectively; Table S1 and Table S2 in the Supporting Information).

(ii) Emission

Solid samples of the imide complexes PtL^1Cl and PtL^2Cl appear bright green and yellow/orange, respectively, when viewed under long-wavelength UV irradiation. Spectra and quantum yields were recorded on powdered samples using an integrating sphere: the emission spectra are shown in Figure 4. The emission maximum of the pyrimidinyl complex PtL^2Cl is displaced towards the red compared to PtL^1Cl, mirroring the trend in absorption, and likely associated with the lower energy π^* orbitals of pyrimidine compared to pyridine rings as described earlier. The quantum yields are are 1.6 and 1.4 % for PtL^1Cl and PtL^2Cl respectively, with lifetimes of 770 and 1000 ns respectively. Lifetimes in the microsecond range are quite typical of phosphorescent Pt(II) complexes {*e.g.*, as in the structurally related, *N^C^N*-coordinated Pt(dpyb)Cl derivatives}, where the formally forbidden $T_1 \rightarrow S_0$ process is facilitated through the SOC effect of the Pt centre. The emission of PtL^3Cl was too weak in the solid state to record a convincing spectrum.

In deoxygenated solution at room temperature, the imide complexes $PtL^{1-2}Cl$ are essentially non-luminescent, presumably due to efficient non-radiative decay processes being opened up in solution compared to the more rigid environment in the solid state. Such a trend has been described in some detail for Ir(III) complexes containing bidentate carbonyl- or imine-based ligands, where the term "enhanced phosphorescence emission in the solid state", or EPESS, has started to be used as a descriptor.[28] Such a situation can, of course, arise in any molecule in which there is significant excited-state distortion that is inhibited by the more rigid environment within the solid compared to solution. The amide complex PtL^3Cl, on the other hand, does show weak luminescence in the red region of the spectrum in solution at room temperature (Figure 5 and Table 1). Nevertheless, the low quantum yield and short lifetime are indicative of fast non-radiative decay processes competing efficiently to deactivate the triplet excited state and render the phosphorescence weak. This complex shows no significant

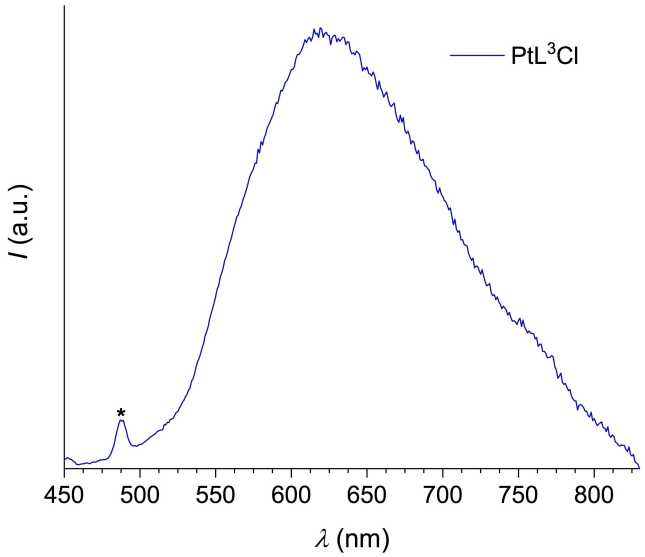

Figure 5. Emission spectrum of PtL^3Cl in CH_2Cl_2 at 295 ± 3 K, $\lambda_{ex} = 430$ nm (* = Raman C–H band of solvent).

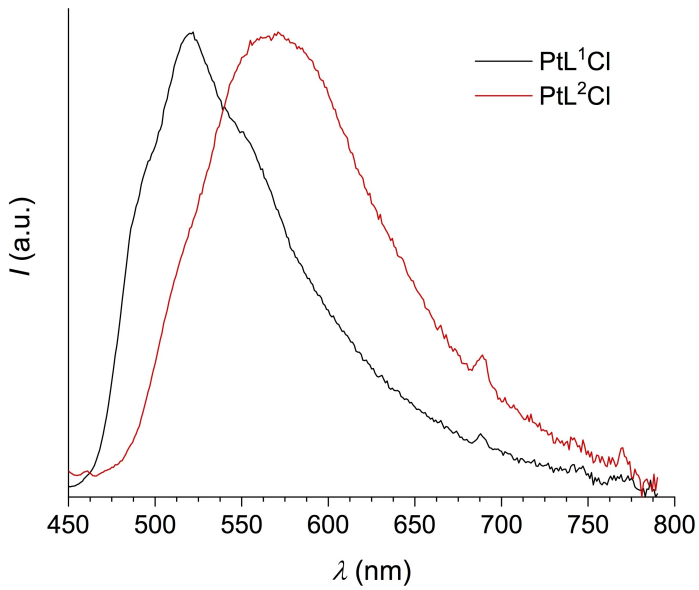

Figure 4. Normalised emission spectra of PtL^1Cl and PtL^2Cl in the solid state at 295 ± 3 K, $\lambda_{ex} = 420$ nm.

Table 1. Luminescence data for $PtL^{1-4}Cl$ in solution at room temperature and in a glass at 77 K.

Complex	Emission at 295 ± 3 [K][a] λ_{max} [nm]	τ/ns[c]	Φ/%[d]	Emission at 77 [K][b] λ_{max} [nm]	τ/[ns]
PtL^1Cl	–[e]	–[e]	–[e]	474, 503, 539, 580	8300
PtL^2Cl	–[e]	–[e]	–[e]	486, 519, 555	5300
PtL^3Cl	622	48 [39]	0.2	563, 599, 643	100
a-PtL^4Cl	624, 683, 745	440 [220]	0.7	627, 687, 738	900
b-PtL^4Cl	535, 567, 605	–[f]	0.2	503, 540, 580	–[f]

[a] In deoxygenated CH_2Cl_2 solution. [b] In diethyl ether/isopentane/ethanol (2:2:1 v/v) for PtL^1Cl–PtL^3Cl, and in butyronitrile for a/b-PtL^4Cl. [c] Corresponding values in air-equilibrated solution are shown in parenthesis. [d] Quantum yields of luminescence determined using $Ru(bpy)_3Cl_2$ in water as the standard. [e] No significant emission was detectable from these complexes in solution at room temperature. For values in the solid state at room temperature, see Figure 4. [f] The lifetime of b-PtL^4Cl was too short for determination using the available equipment, the intensity being too weak to reliably deconvolve the decay from the instrument response function.

emission in the solid state, in contrast to $PtL^{1-2}Cl$, presumably due to deactivation pathways that involve *inter*molecular interactions. In dilute glassy solution at 77 K, all three complexes $PtL^{1-3}Cl$ are weakly emissive, with some vibrational structure evident in the spectra (Figure S11 and Table 1).

We note that PdL^1Cl, the palladium analogue of PtL^1Cl, has previously been prepared and structurally characterised, but no emission properties were reported for that material.[29] In most cases, Pd(II) complexes do not show significant phosphorescence at room temperature where their Pt(II) analogues may do so. The superiority of Pt(II) in this respect has two origins. Firstly, the stronger ligand field associated with platinum may help raise potentially deactivating d–d states to thermally less accessible energies, reducing their ability to act as a quenching pathway for the emissive excited states. Secondly, the higher spin-orbit coupling of Pt compared to Pd facilitates the formally forbidden $T_1 \rightarrow S_0$ transition.[2]

The pair of isomeric hydrazide complexes *a/b*-PtL^4Cl are both weakly luminescent in solution at room temperature (Figure 6 and Table 1). The isomer *a*-PtL^4Cl displays a vibrationally structured spectrum. Such structured spectra, when observed under ambient conditions, tend to be associated with excited states of predominantly π–π* character, as opposed to CT. The component band of highest intensity is the 0,0 band, indicative of little distortion between the emissive excited state and the ground state and hence a highly rigid chromophoric unit. In line with this interpretation, the corresponding spectrum at 77 K is very similar to that at room temperature, with no significant shift of the vibrational band maxima. The luminescence lifetime is 440 ns in deoxygenated solution, which is again consistent with formally forbidden phosphorescence from the triplet excited state facilitated by the Pt(II) centre. The lifetime falls to 220 ns under air-equilibrated conditions, from which the bimolecular rate constant for quenching by O_2 may

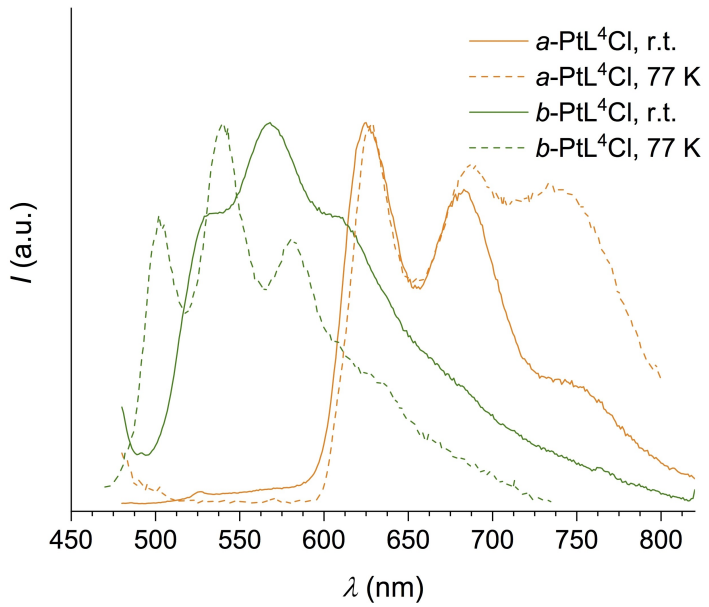

Figure 6. Normalised emission spectra of a-PtL^4Cl and b-PtL^4Cl in CH_2Cl_2 at 295 ± 3 K (solid orange and green lines respectively), and corresponding spectra at 77 K in EPA (dashed lines).

be estimated to be $1.0\times10^9\ M^{-1}s^{-1}$, a value quite typical of phosphorescent metal complexes with molecular weights around 500 g mol^{-1}, such as those based on Pt(dpyb)Cl.[11d]

The complex *b*-PtL^{4}Cl emits at much shorter wavelengths than its isomer. Based on the wavelengths of the 0,0 bands (624 and 535 nm for *a* and *b* respectively), the difference in energy between the emissive excited states of the two complexes is estimated to be 2700 cm^{-1}. The vibrational structure in the room temperature spectrum of the *b* form is less well-resolved than the *a* isomer and, unlike the *a* isomer, it shows a modest shift to the blue on going to 77 K, of around 1200 cm^{-1}. Both observations suggest a higher degree of excited state distortion for the *b* isomer and thus perhaps to an excited state of different character. For this isomer, the lifetime proved too short for detection with the available equipment, probably <1 ns, and indeed the emission in solution was not detectably quenched upon aeration, an observation that also points to the lifetime being short. Finally, it may be noted that the Stokes' shift of this complex is particularly small: its absorption spectrum tails to around 530 nm, a value remarkably similar to the 0,0 band of the emission spectrum. Taken together, these observations strongly suggest that the observed emission of *b*-PtL^{4}Cl is due to *fluorescence* from the S_1 state as opposed to the T_1 phosphorescence observed for *a*-PtL^{4}Cl.

To provide further insight into this remarkable and unexpected difference, the $S_1\rightarrow S_0$ fluorescence and $T_1\rightarrow S_0$ phosphorescence spectra of the two isomeric complexes were calculated at the CAM-B3LYP/Def2-TZVP level of theory (Figure S10). The calculated phosphorescence spectrum of *a*-PtL^{4}Cl closely matches (in energy) the experimentally observed emission, whereas for the *b* isomer, the observed emission falls in the calculated fluorescence region. Thus, it appears that the lowest-energy singlet states of the two isomers have similar character (hydrazide-localised $^1\pi$–π^* state, *vide supra*, Figure S3 and Figure S4 and Table S1) and energies, based on their similar lowest-energy absorption bands (Figure 3), but their triplet state energies differ. The large S_1–T_1 energy gap for *b*-PtL^{4}Cl (Figure S10) probably serves to diminish the rate of $S_1\rightarrow T_1$ intersystem crossing (inversely proportional to the energy gap[5]) such that S_1 fluorescence is observed for this isomer. It is also likely that there is less metal character in the singlet excited state of the *b* isomer compared to the *a* (Figure S3 and Figure S4) which would further contribute to limiting the rate of intersystem crossing.

No phosphorescence was reported for the related Pd(II) complexes previously reported,[25] in contrast to our newly prepared Pt(II) complexes of ligand L^4. As noted earlier, potentially emissive ligand-centred or charge-transfer excited states in Pd(II) complexes are normally subject to more efficient non-radiative decay processes, owing to low-lying d-d states arising from the weaker ligand field associated with Pd(II), whilst the spin-orbit coupling effect of Pd is also weaker.

Photophysical properties of the dinuclear complexes

The conversion of PtL^{4}Cl to the bimetallic Pt–Ru complex PtCl(μ-L^4)RuCl$_2$(PPh$_3$)$_2$ is accompanied by the appearance of a relatively intense absorption band at long wavelength, $\lambda_{max}=$ 677 nm (Figure 7). The band is most likely due to an MLCT transition from the Ru(II) centre to the bridging L^4 ligand. A low-energy band was also observed by Nakajima and co-workers in their corresponding Pd–Ru complex, albeit at somewhat longer wavelength beyond 700 nm.[27] The well-defined band present at 473 nm in *a*-PtL^{4}Cl is slightly blue-shifted (455 nm) in the Pt–Ru complex, suggesting that the d(Pt)$\rightarrow\pi^*$(L^4) transition is somewhat raised in energy upon coordination of Ru(II), probably owing to a small destabilisation of the π^* orbitals on

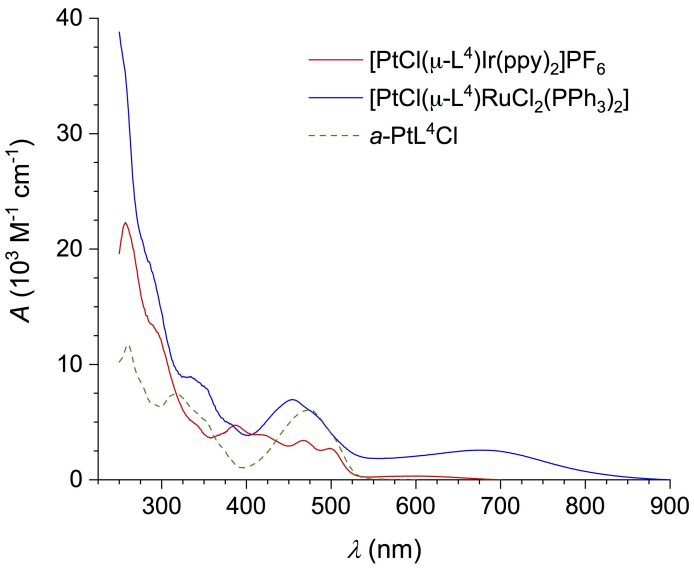

Figure 7. Absorption spectra of [PtCl(μ-L^4)RuCl$_2$(PPh$_3$)$_2$] (red line) and [PtCl(μ-L^4)Ir(ppy)$_2$]PF$_6$ (blue line) in CH$_2$Cl$_2$ at 298 ± 3 K, together with the spectrum of a-PtL^{4}Cl for comparison (dashed green line)

L^4. The dinuclear complex $[PtCl(\mu\text{-}L^4)Ir(ppy)_2]PF_6$ also has bands in the 400–500 nm region that can reasonably be attributed to those typically observed in this region for $Ir(ppy)_2$ derivatives, superimposed on the visible absorption band associated with the Pt unit. In addition, a weak, low-energy, broad band centred around 600 nm is apparent.

Neither of these bimetallic complexes shows detectable luminescence at room temperature. For the Ru–Pt complex, this observation is in line with other studies where low-energy absorbing RuL_4X_2 units efficiently quench the excited states of covalently linked higher-energy emitters.[30] Whilst many $Ir(ppy)_2(L^{\wedge}X)$-based complexes are brightly emissive, those with ancillary $L^{\wedge}X$ ligands having low-energy excited states associated with them are often not so. A well-known example is that of $Ir(ppy)_2(O^{\wedge}O\text{-dbm})$ (dbm = dibenzoylmethane), where the lack of emission is attributed to vibrational quenching in the low-frequency region of the conjugated $O^{\wedge}O$ ligand.[31] It seems likely that a similar effect may be at work in the present instance.

Concluding Remarks

This work demonstrates that platinum(II) complexes of pincer ligands featuring N^- central ligating atoms – formed by deprotonation of imide, amide or hydrazide units – can be prepared readily from corresponding proligands. The proligands HL^3 and HL^4 are available via simple condensation reactions from a standard organic compound – ethylpicolinate – whilst HL^1 is likewise prepared easily by hydrolysis of low-cost tripyridyltriazine. The ease of synthesis and lack of requirement for expensive organometallic reagents or palladium catalysts contrasts with routes typically used to prepare related cyclometallating pincer ligands – featuring a central carbon in place of nitrogen – such as 1,3-dipyridylbenzene (dpyb) and its derivatives.[14]

The resulting Pt(II) complexes featuring the ligands bound in a tridentate manner – with a monodentate chloride ligand completing the coordination sphere – do show luminescence, albeit much weaker than that displayed by Pt(dpyb)Cl. The imide complexes display green or green-yellow phosphorescence in the solid-state, but the emission is largely quenched in solution at ambient temperature, due to efficient non-radiative decay processes being introduced. In contrast, PtL^3Cl – the amide analogue of imide PtL^1Cl featuring only one C=O unit – shows weak red phosphorescence in solution, with the shift to lower energy likely due to a destabilisation of the highest occupied orbitals. PtL^4Cl can exist as two isomers, both of which are luminescent in solution with modest quantum yields. The "amide-N-bound" *a* form is red-shifted compared to the "imine-N-bound" *b* isomer and it emerges that the emission has an unexpectedly different origin in the two cases. The '*a* form' displays phosphorescence from the triplet state, whereas the origin of the '*b* form' emission is fluorescence, as supported both by DFT calculations and by the short emission lifetime and insensitivity of the emission to dissolved oxygen. This represents a highly unusual case of isomerism determining the singlet versus triplet nature of emission in a metal complex.

Whilst the luminescence performance of these first examples of $N^{\wedge}N^{\wedge}N$-bound Pt(II) complexes are inferior to the cyclometallated systems, it may be anticipated that modifications to these core structures may lead to significant improvements. For example, from the well-known precedent of $[Pt(tpy)Cl]^+$ and Pt(phbpy)Cl and their derivatives (tpy = terpyridine, phbpy = 6-phenylbipyridine), the metathesis of the chloride ligand to strong-field ligands such as acetylides may help to increase the metal character in the excited state, particularly for the complexes of PtL^4Cl, and thus promote the radiative decay rate.[32] Similarly, the appendage of an additional ligating unit, such as a phenolate, into the structures to generate a *tetradentate* ligand may confer the additional rigidity necessary to limit non-radiative decay pathways.[33] The presence of additional, potentially bidentate ligating units in the resulting complexes renders them of potential interest in the generation of multimetallic structures, as exemplified here by the formation of two heterodinuclear complexes incorporating the *a*-PtL^4Cl unit bound to Ru(II) or Ir(III).

Experimental Section

^1H and ^{13}C NMR spectra were recorded on Varian or Bruker instruments at the frequencies indicated. Chemical shifts (δ) are in ppm, referenced relative to residual protio-solvent resonances, and coupling constants (*J*) are in hertz. All solvents used in the preparative work were of at least analytical reagent grade, and water was purified using the Purite system. Solvents used for optical spectroscopy were HPLC grade. Proligands $HL^{1–4}$ were prepared broadly following procedures described elsewhere.[18,23,24] The platinum precursor $Pt(COD)Cl_2$ was prepared by a standard procedure.[34]

PtL^1Cl

$Pt(COD)Cl_2$ (83 mg, 0.22 mmol) and NEt_3 (22 mg, 0.22 mmol) were added to a solution of HL^1 (50 mg, 0.22 mmol) in MeCN (2 mL) and the mixture was stirred at 60 °C under argon for 18 h. The resulting yellow suspension was filtered and the solid was washed with MeCN (5 × 5 mL) and dried under vacuum to yield the title compound as a bright yellow solid (65 mg, 64 %). The ^1H NMR and MS data were consistent with those previously reported by Miguel *et al.*[20] UV/Vis (CH_2Cl_2): λ_{max} (ε) = 262sh (14000), 328 (5710), 389 (2760), 408sh nm (2520 $M^{-1}cm^{-1}$). Elemental analysis calcd (%) for $C_{12}H_8N_3O_2ClPt$ (rigorously dried material): C 31.6, H 1.8, N 9.2; found C 31.3, H 2.2, N 8.9.

PtL^2Cl

A mixture of HL^2 (150 mg, 0.65 mmol) and K_2PtCl_4 (272 mg, 0.65 mmol) in DMF (10 mL) was stirred at 60 °C under argon for 24 h. The resulting orange suspension was filtered. Water (10 mL) was added to the filtrate, which was then extracted into DCM (3 × 20 mL). The solvent was removed under reduced pressure to give a dark orange solid, which was recrystallized from DMSO to yield the product as a yellow solid (10 mg, 3 %). ^1H NMR (700 MHz, DMSO-d_6): δ = 9.32 (d, J = 5.0, $J(^{195}Pt–^1H)$ = 38, 4H; H^4 and H^6), 7.96 ppm (t, J = 5.0, 2H; H^5). The material was not sufficiently soluble to obtain a ^{13}C NMR spectrum. IR (solid, ATR): ν = 3593 (w), 1742 (s), 1654 (m), 1582

(m), 1368 (w), 1341 (s), 1305 (w), 1274 (w), 1190 (w), 1033 (w), 696 (s), 676 (m), 666 (m), 506 (w) cm^{-1}; UV/Vis (CH_2Cl_2): λ_{max} (ε) = 270sh (9240), 334 (4310), 401 (1920), 432sh nm (1480 $M^{-1}cm^{-1}$). MS (ES+): *m/z:* 459 $[M+H]^+$; HRMS (ES+): *m/z* calcd for $[C_{10}H_7N_5O_2{}^{194}PtCl]^+$: 457.9915 $[M+H]^+$; found: 457.9919. Elemental analysis calcd (%) for $C_{10}H_6N_5O_2ClPt.(CH_3)_2SO$: C 26.9, H 2.3, N 13.1; found C 27.4, H 2.5, N 12.7.

PtL^3Cl

$Pt(COD)Cl_2$ (53 mg, 0.14 mmol) and NEt_3 (14 mg, 0.14 mmol) were added to a solution of HL^3 (30 mg, 0.14 mmol) in MeCN (2 mL) and the mixture was stirred at 60 °C under argon for 18 h. The resulting yellow slurry was filtered and the solid was washed with MeCN (5× 5 mL) and dried under vacuum to yield the title compound as a bright yellow solid (24 mg, 41 %). ^{1}H NMR (700 MHz, $CDCl_3$): δ = 9.13 (d, *J* = 5.5, 1H; $H^{6'}$), 9.02 (d, *J* = 5.5, 1H; H^6), 8.02 (td, *J* = 8.0 and 1.5, 1H; H^5), 7.94 (td, *J* = 8.0 and 1.5, 1H; $H^{5'}$), 7.81 (d, *J* = 8.0, 1H; H^3), 7.48 (ddd, *J* = 8.0, 5.5 and 2.0, 1H; H^4), 7.42 (d, *J* = 8.0, 1H; $H^{3'}$), 7.30 (t, *J* = 7.0, 1H; $H^{4'}$), 5.07 ppm (s, 2H; H^{CH2}). Primed resonances indicate the py–CH=N ring; non-primed the py–CO ring. ^{13}C NMR (176 MHz, $CDCl_3$): δ = 169.5 ($C^{2'}$), 168.4 ($C^{C=O}$), 157.9 (C^2), 150.0 ($C^{6'}$), 149.5 (C^6), 139.9 (C^5), 138.7 ($C^{5'}$), 127.2 (C^4), 125.7 (C^3), 123.7 ($C^{9'}$), 122.3 ($C^{3'}$), 55.0 ppm (C^{CH2}). The IR data are consistent with those previously reported by Miguel *et al.*[20] UV/Vis (CH_2Cl_2): λ_{max}(ε) = 266 (9430), 324 (5200), 415 nm (1640 $M^{-1}cm^{-1}$). MS(ES+): *m/z* 443 $[M+H]^+$; HRMS (ES+): *m/z* calcd for $[C_{12}H_{11}N_3O^{194}PtCl]^+$: 442.0217 $[M+H]^+$; found: 442.0227. Elemental analysis calcd (%) for $C_{12}H_{10}N_3OClPt$ (rigorously dried material): C 32.6, H 2.3, N 9.5; found C 32.2, H 2.5, N 9.2.

PtL^4Cl

A solution of HL^4 (91 mg, 0.40 mmol), $Pt(COD)Cl_2$ (150 mg, 0.4 mmol) and NEt_3 (41 mg, 0.40 mmol) in MeCN (6 mL) was refluxed under argon for 48 h, after which a purple solid was isolated by filtration of the reaction mixture. The solid material was loaded onto silica gel in DCM and purified by column chromatography (5 % MeOH/DCM) to give, after removal of solvent from the respective fractions, *a*-PtL^4Cl as a burnt-orange solid (51 mg, 28 %) and *b*-PtL^4Cl as a dark purple solid (27 mg, 15 %).

Data for *a*-$PtL^{22}Cl$: R_f = 0.3. ^{1}H NMR (600 MHz, DMSO-d_6): δ = 10.0 (d, *J* = 6, 1H,; $H^{6'}$, no ^{195}Pt satellites observed in this solvent), 9.39 (d, *J* = 6.0, 1H; H^6), 8.29–8.26 (m, H^4 and $H^{4'}$, 2H), 7.98 (dd, *J* = 8.0 and 1.0, 1H; H^3), 7.89 (dd, *J* = 8.0 and 1.0, 1H; $H^{3'}$), 7.81 (ddd, *J* = 7.5, 6.0 and 1.5, 1H; H^5), 7.73 (s, 1H; H^{imine}), 7.55 ppm (ddd, *J* = 7.0, 6.0 and 1.5, 1H; $H^{5'}$). ^{13}C NMR (DMSO-d_6, 151 MHz): δ = 170.3 ($C^{C=O}$), 151.9 ($C^{6'}$), 149.4 ($C^{2'}$), 149.3 (C^6), 141.7 ($C^{4'}$ or C^4), 140.1 ($C^{4'}$ or C^4), 136.7 (C^2), 136.7 (C^{imine}), 129.6 ($C^{3'}$), 129.1 (C^5), 126.3 (C^3), 124.9 ppm ($C^{5'}$). IR (solid): 1682 (m), 1605 (w), 1484 (w), 1316 (m), 1303 (m), 1284 (s), 1168 (w), 1154 (m), 1124 (w), 1105 (w), 765 (s), 757 (m), 731 (m), 676 (s), 580 (m), 521 (w), 470 (w), 440 (m) cm^{-1}. UV/Vis (CH_2Cl_2): λ_{max} (ε) = 260 (11700), 316 (7440), 473 nm (6040 $M^{-1}cm^{-1}$). MS (ES+): *m/z* 457 $[M+H]^+$. HRMS (ES+): *m/z* 455.0211 $[M]^+$; calculated for $[C_{12}H_{10}N_4O^{194}PtCl]^+$ 455.0170.

Data for *b*-$PtL^{22}Cl$: R_f = 0.2. ^{1}H NMR ($CDCl_3$, 400 MHz): δ_H = 9.97 (dd, *J* = 6.0 and 1.5, $J(^{195}Pt–^1H)$ = 39, 1H; $H^{6'}$), 9.39 (d, *J* = 6.0, $J(^{195}Pt)$ = 39.0, 1H; H^6), 9.04 (dd, *J* = 8.5 and 2, 1H; H^3), 8.36 (s, 1H; H^{imine}), 8.10 (dt, *J* = 8.0 and 2.0, 1H; H^4 or $H^{4'}$), 7.90 (dt, *J* = 8.0 and 1.5, 1H; H^4 or $H^{4'}$), 7.50–7.44 (m, 2H; H^5 and $H^{3'}$), 7.32 ppm (ddd, *J* = 8.0, 6.0 and 1.5, 1H; $H^{5'}$). The material was not sufficiently soluble to obtain a ^{13}C NMR spectrum. IR (solid): 1572 (w), 1553 (m), 1498 (s), 1435 (w), 1373 (s), 1319 (m), 1188 (w), 1162 (m), 764 (m), 755 (s), 669 (m), 614 (w) cm^{-1}. UV/Vis (CH_2Cl_2): λ_{max} (ε) = 264 (9810), 291 (13900), 320 (10100), 379 (9660), 468 nm (10500 $M^{-1}cm^{-1}$). MS (ES+): *m/z* 457 $[M+H]^+$; HRMS (ASAP+): *m/z* 455.0175 $[M]^+$; calculated for $[C_{12}H_{10}N_4O^{194}PtCl]^+$ 455.0170.

[*a*-PtCl(μ-L^4)Ir(ppy)$_2$]PF_6

$[Ir(ppy)_2(\mu\text{-}Cl)]_2$ (12 mg, 0.011 mmol) and *a*-PtL^4Cl (10 mg, 0.022 mmol) were heated in a MeOH/DCM mixture (6:5 v/v, 2.2 mL) at 65 °C for 2 h, after which the solvent was removed under vacuum. The residue was dissolved the minimum volume of MeCN/H_2O (1:1 v/v) and the resulting solution was added dropwise to a saturated aqueous solution of KPF_6 (5 mL). The resulting precipitate was separated by centrifugation and washed with water (3×5 mL) to give the dimetallic product as a green solid (20 mg, 82 %). ^{1}H NMR ($(CD_3)_2CO$, 600 MHz): 10.17 (dd, *J* = 8.0 and 1.5; 1H), 9.54 (ddd, *J* = 6.0, 1.5 and 0.5; 1H), 8.80 (ddd, *J* = 6.0, 1.5 and 1.0; 1H), 8.67 (ddd, *J* = 6.0, 1.5 and 1.0; 1H), 8.39 (td, *J* = 8.0 and 1.5, 1H), 8.29 (td, *J* = 8.0 and 1.5, 1H), 8.27–8.25 (m, 2H), 8.22 (dd, *J* = 8.0 and 1.5, 1H), 8.07–8.04 (m, 2H), 8.01 (ddd, *J* = 8.0, 6.0 and 1.5, 1H), 7.85 (td, *J* = 8.0 and 1.0, 2H), 7.73 (ddd, J = 7.5, 6.0 and 1.5, 1H), 7.48 (dd, *J* = 8.0 and 1.5, 1H), 7.39 (ddd, *J* = 7.0, 6.0 and 1.5, 1H), 7.34 (ddd, *J* = 7.5, 6.0 and 1.5, 1H), 7.30 (s, 1H), 7.01 (td, *J* = 7.5 and 1.0, 1H), 6.97 (td, *J* = 7.5 and 1.0, 1H), 6.87 (td, *J* = 7.5 and 1.0, 1H), 6.83 (td, *J* = 7.5 and 1.0, 1H), 6.32 (dd, *J* = 8.0 and 1.0, 1H), 6.18 ppm (dd, *J* = 7.5 and 1.0, 1H). ^{13}C NMR ($(CD_3)_2CO$, 151 MHz): 167.8, 166.9, 158.3, 153.4, 150.9, 150.2, 149.3, 147.9, 147.6, 144.9, 144.0, 142.3, 140.9, 139.8, 139.2, 139.0, 133.0, 132.4, 131.7, 130.3, 130.1, 129.5, 128.0, 127.8, 124.9, 124.4, 123.5, 122.7, 122.5, 119.9, 119.6 ppm. IR (solid): 1605 (w), 1570 (w), 1481 (m), 1374 (w), 1300 (w), 833 (s), 798 (m), 764 (m), 753 (s), 764 (m), 753 (s), 733 (m), 680 (w), 670 (w), 556 (s), 467 (w), 419 (w) cm^{-1}. UV/Vis (CH_2Cl_2): λ_{max} (ε) = 335sh (5100), 387 (4720), 415 (3920), 467 (3410), 498 (2700), 600 nm (323 $M^{-1}cm^{-1}$). MS (ES+): *m/z* 956 $[M]^+$; HRMS (ES+): *m/z* 955.1071 $[M]^+$; calculated for $[C_{34}H_{25}N_6OCl^{194}PtIr]^+$ 955.1033.

a-PtCl(μ-L^4)$RuCl_2(PPh_3)_2$

A mixture of *a*-PtL^4Cl (20 mg, 0.04 mmol) and $RuCl_2(PPh_3)_3$ (42 mg, 0.04 mmol) in DCM (7 mL) was stirred for 4 h. The resulting solution was reduced to approximately 2.5 mL by evaporation of solvent under reduced pressure, and hexane (9 mL) added leading to precipitation. The suspension was filtered to yield the product as a dark green solid (41 mg, 75 %). ^{1}H NMR ($CDCl_3$, 600 MHz): 10.06 (d, *J* = 6.5, 1H), 9.41 (d, *J* = 6.0, 1H), 7.92 (td, *J* = 8.0 and 1.0, 1H), 7.85 (d, *J* = 3.0, 1H), 7.71 (td, *J* = 7.5 and 1.0, 1H), 7.67–7.64 (m, 6H), 7.55 (d, *J* = 8.0, 1H), 7.49 (ddd, *J* = 7.5, 5.5 and 1.0, 1H), 7.47–7.43 (m, 6H), 7.25–7.22 (m, 6H), 7.20 (ddd, *J* = 7.0, 6.0 and 1.5, 1H), 7.16–7.13 (m, 6H), 7.06–7.02 (m, 6H), 6.13 ppm (d, 1H, *J* = 8.0). IR/cm^{-1}: 1607 m, 1583 w, 1569 w, 1482 m, 1431 m, 1384 m, 1298 m, 1090 m, 753 m, 693 s, 672 m, 535 s, 522 vs, 500 s, 464 m, 426 m, 412 m. UV/Vis (CH_2Cl_2): λ_{max}(ε) = 332(8920), 380sh (4830), 455 (6940), 677 nm (2570 $M^{-1}cm^{-1}$). MS (ES+): *m/z* 1117 $[M(-Cl)+H]^+$; HRMS (ES+): *m/z* 1112.0632 $[M-Cl]^+$; calculated for $[C_{48}H_{39}N_4OP_2Cl_2{}^{99}Ru^{194}Pt]^+$ 1112.0662. Elemental analysis calcd (%) for $C_{48}H_{39}N_4OP_2Cl_3RuPt$: C 49.21; H 3.42; N 5.12; found: C 50.03, H 3.41, N 4.86.

Photophysical measurements

Absorption spectra in solution were measured on a Biotek Instruments XS spectrometer, using quartz cuvettes of 1 cm path length. Samples for emission measurements were contained within quartz cuvettes of 1 cm path length modified to allow connection to a high-vacuum line. Degassing was achieved *via* a minimum of three freeze-pump-thaw cycles whilst connected to the vacuum manifold; final vapour pressure at 77 K was $< 5\times10^{-2}$ mbar, as monitored using a Pirani gauge. Spectra were recorded on a Jobin Yvon

Fluoromax-2 spectrofluorimeter with an R928 PMT detector and corrected for the wavelength dependence of the monochromator and detector. Luminescence quantum yields were determined using $[Ru(bpy)_3]Cl_2$ in aqueous solution as the standard ($\Phi = 0.040$).[35] The luminescence lifetimes of the complexes (both in solution and solid state) were measured by time-correlated single photon counting (TCSPC), following excitation at 404 nm with a pulsed diode laser. The emitted light was detected at 90° geometry using a Peltier-cooled R928 PMT after passage through a monochromator. The estimated uncertainty in the quoted lifetimes is ±10% or better. Spectra at 77 K were recorded in a glass of EPA (diethyl ether/isopentane/ethanol, 2:2:1 v/v) or butyronitrile. The spectra and quantum yields of solid state samples were recorded using a Jobin Yvon Quanta-Φ integrating sphere operated in conjunction with a Fluorolog spectrometer.

DFT Calculations

The studied molecules were optimized in Gaussian 16[36] to the corresponding minimum (S_0 or S_1 state), which was confirmed by frequency calculations having no imaginary frequency. The CAM-B3LYP functional[37] was used for the optimization together with the Def2-TZVP basis set and C-PCM model for dichloromethane solvent. Atomic coordinates of the optimized geometries in *xyz* format are listed in Section 4 of the Supporting Information.

Absorption, fluorescence, and phosphorescence spectra were calculated using the Dalton program.[38] For this purpose, the S_0 geometry (for absorption and phosphorescence spectra) and S_1 geometry (for fluorescence spectra) derived from previous calculations using CAM-B3LYP were used. For the absorption spectra, the first 20 excited states were considered. For fluorescence spectra, the five lowest excited states were taken into account, whilst for phosphorescence, the lowest triplet state was used. Relativistic effects were taken into account by the use of effective charge spin-orbit integrals. The CAM-B3LYP DFT functional was used with the Def2-TZVP basis set and an effective core potential (ECP) for the platinum atom. The PCM model with non-equilibrium solvation was utilized to model dichloromethane as a solvent. Almost identical results were obtained using the Douglas-Kroll method, with the atomic mean-field spin-orbit integral approximation, the CAM-B3LYP functional, ANO-DK3 basis set (6s 4p 3d 1f) for platinum, and cc-pVTZ-DK for all other elements.

The calculated spectra were simulated with half-widths of 0.1511 eV (1210 cm^{-1}) for absorption and 0.25 eV (2020 cm^{-1}) for emission spectra. Energies were scaled by 0.815 for better comparison between predicted and experimental spectra. For comparison, and to provide further confidence in the validity of the results, the absorption spectra were also calculated in Gaussian 16 with the use of the BMK,[39] CAM-B3LYP and ωB97X-D[40] DFT functionals, Def2-TZVP basis set and C-PCM model for dichloromethane. All the methods gave similar results, as summarised in Figures S5–S9.

Supporting Information (see footnote on the first page of this article): ^{1}H NMR spectral comparison with Pd(II) complexes; ^{1}H NMR and high-resolution mass spectra of complexes; representative frontier orbital plots; simulated absorption spectra of $PtL^{1-4}Cl$ and emission spectra of *a/b*-PtL^4Cl calculated by TD-DFT; additional spectra at 77 K, calculated *xyz* atomic coordinates of the energy-minimised structures.

Acknowledgements

We thank EPSRC and Durham University for support. Computational resources were supplied by the project "e-Infrastruktura CZ" (e-INFRA LM2018140) provided within the program "Projects of Large Research, Development and Innovations Infrastructures."

Conflict of Interest

The authors declare no conflict of interest.

Keywords: Platinum · Luminescence · Coordination modes · Hydrazones · Photochemistry

[1] a) The Chemistry of Pincer Compounds ed. D. Morales-Morales, C. Jensen, Elsevier, **2007**; b) *Organometallic Pincer Chemistry*, G. Van Koten, D. Milstein (eds), *Top. Organomet. Chem.* **2013**, *40*; c) M. Albrecht, G. van Koten, *Angew. Chem. Int. Ed.* **2001**, *40*, 3750; d) M. Albrecht, D. Morales-Morales, *Pincer-Type Iridium Complexes for Organic Transformations in: L. A. Oro, C. Claver (eds). Iridium Complexes in Organic Synthesis.* Weinheim: Wiley-VCH, **2009**; e) M. C. Haibach, D. Y. Wang, T. J. Emge, K. Krogh-Jespersen, A. S. Goldman, *Chem. Sci.* **2013**, *4*, 3683–3692.

[2] G. R. Freeman, J. A. G. Williams, *Top. Organomet. Chem.* **2013**, *40*, 89–130.

[3] a) D. C. Babbini, V. M. Iluc, *Organometallics* **2015**, *34*, 3141–3151; b) P. M. P. Garcia, T. Di Franco, A. Epenoy, R. Scopelliti, X. L. Hu, *ACS Catal.* **2016**, *6*, 258–261.

[4] a) D. R. McMillin, J. J. Moore, *Coord. Chem. Rev.* **2002**, *229*, 113–121; b) J. A. G. Williams, *Top. Curr. Chem.* **2007**, *281*, 205–268; c) R. McGuire, M. C. McGuire, D. R. McMillin, *Coord. Chem. Rev.* **2010**, *254*, 2574–2583; d) L. Murphy, J. A. G. Williams, *Top. Organomet. Chem.*, **2010**, *28*, 75–111; e) Y. Chi, P. T. Chou, *Chem. Soc. Rev.* **2010**, *39*, 638–655; f) Y. Unger, D. Meyer, O. Molt, C. Schildknecht, I. Munster, G. Wagenblast, T. Strassner, *Angew. Chem. Int. Ed.* **2010**, *49*, 10214–10216; *Angew. Chem.* **2010**, *122*, 10412–10414; g) A. Diez, E. Lalinde, M. T. Moreno, *Coord. Chem. Rev.* **2011**, *255*, 2426–2447; h) S. Q. Huo, J. Carroll, D. K. Vezzu, *Asian J. Org. Chem.* **2015**, *4*, 1210–1245; i) K. Li, G. S. M. Tong, Q. Y. Wan, G. Cheng, W. Y. Tong, W. H. Ang, W. L. Kwong, C. M. Che, *Chem. Sci.* **2016**, *7*, 1653–1673; j) J. Soellner, M. Tenne, G. Wagenblast, T. Strassner, *Chem. Eur. J.* **2016**, *22*, 9914–9918; k) M. Krause, D. Kourkoulos, D. Gonzalez-Abradelo, K. Meerholz, C. A. Strassert, A Klein, *Eur. J. Inorg. Chem.* **2017**, *44*, 5215–5223; l) C. Cebrian, M. Mauro, *Beilstein J. Org. Chem.* **2018**, *14*, 1459–1481; m) A. Haque, L. L. Xu, R. A. Al-Bushi, M. K. Al-Suti, R. Ilmi, Z. L. Guo, M. S. Khan, W. Y. Wong, P. R. Raithby, *Chem. Soc. Rev.* **2019**, *48*, 5547–5563; n) V. W.-W. Yam, A. S.-Y. Law, *Coord. Chem. Rev.* **2020**, *414*, 213298.

[5] H. Yersin, A. F. Rausch, R. Czerwieniec, T. Hofbeck, T. Fischer, *Coord. Chem. Rev.* **2011**, *255*, 2622–2652.

[6] a) Q. Zhao, C. Huang, F. Li, *Chem. Soc. Rev.* **2011**, *40*, 2508–2524; b) K. K. W. Lo, A. W. T. Choi, W. H. T. Law, *Dalton Trans.* **2012**, *41*, 6021–6047; c) E. Baggaley, J. A. Weinstein, J. A. G. Williams, *Coord. Chem. Rev.* **2012**, *256*, 1762–1785; d) E. Baggaley, J. A. Weinstein, J. A. G. Williams, *Struct. Bond.* **2015**, *165*, 205–256.

[7] a) Q. Z. Yang, L. Z. Wu, H. Zhang, B. Chen, Z. X. Wu, L. P. Zhang, C. H. Tung, *Inorg. Chem.* **2004**, *43*, 5195–5197; b) W. S. Tang, X. X. Lu, K. M. C. Wong, V. W. W. Yam, *J. Mater. Chem.* **2005**, *15*, 2714–2720; c) C. Yu, K. H. Y. Chan, K. M. C. Wong, V. W. W. Yam, *Proc. Natl. Acad. Sci. USA* **2006**, *103*, 19652–19657; d) P.-H. Lanoë, J.-L. Fillaut, L. Toupet, J. A. G. Williams, H. Le Bozec, V. Guerchais, *Chem. Commun.* **2008**, 4333–4335; e) Q. Zhao, F. Li, C. Huang, *Chem. Soc. Rev.* **2010**, *39*, 3007–3030.

[8] a) W. Y. Wong, C. L. Ho, *J. Mater. Chem.* **2009**, *19*, 4457–4482; b) C. M. Che, C. C. Kwok, S. W. Lai, A. F. Rausch, W. J. Finkenzeller, N. Y. Zhu, H. Yersin, *Chem. Eur. J.* **2010**, *16*, 233–247; c) J. Kalinowski, V. Fattori, M. Cocchi, J. A. G. Williams, *Coord. Chem. Rev.* **2011**, *255*, 2401–2425; d) C. Cebrian, M. Mauro, D. Kouroulos, P. Mercandelli, D. Hertel, K. Meerholz, C. A. Strassert, L. De Cola, *Adv. Mater.* **2013**, *25*, 437–442; e) M.-C. Tang, A. K.-W. Chan, M.-Y. Chan, V. W.-W. Yam, *Top. Curr. Chem.* **2016**, *374*, 46.

[9] a) V. Adamovich, J. Brooks, A. Tamayo, A. M. Alexander, P. I. Djurovich, B. W. D'Andrade, C. Adachi, S. R. Forrest, M. E. Thompson, *New J. Chem.* **2002**, *26*, 1171–1178; b) M. Cocchi, J. Kalinowski, D. Virgili, J. A. G. Williams, *Appl. Phys. Lett.* **2008**, *92*, 113302; c) K. T. Ly, R. W. Chen-Cheng, H.-W. Lin, Y.-J. Shiau, S.-H. Liu, P.-T. Chou, C.-S. Tsao, Y.-C. Huang, Y. Chi, *Nat. Photonics* **2017**, *11*, 63–68.
[10] a) G. S. M. Tong, C. M. Che, *Chem. Eur. J.* **2009**, *15*, 7225–7237; b) A. F. Rausch, L. Murphy, J. A. G. Williams, H. Yersin, *Inorg. Chem.* **2012**, *51*, 312–319.
[11] a) J. A. G. Williams, A. Beeby, E. Stephen Davies, J. A. Weinstein, C. Wilson, *Inorg. Chem.* **2003**, *42*, 8609–8611; b) S. J. Farley, D. L. Rochester, A. L. Thompson, J. A. K. Howard, J. A. G. Williams, *Inorg. Chem.* **2005**, *44*, 9690–9703; c) V. N. Kozhevnikov, B. Donnio, D. W. Bruce, *Angew. Chem. Int. Ed.* **2008**, *47*, 6286–6289; *Angew. Chem.* **2008**, *120*, 6382–6385; d) D. L. Rochester, S. Develay, S. Záliš, J. A. G. Williams, *Dalton Trans.* **2009**, 1728–1741; e) W. A. Tarran, G. R. Freeman, L. Murphy, A. M. Benham, R. Kataky, J. A. G. Williams, *Inorg. Chem.* **2014**, *53*, 5738–5749; f) A. Y. Y. Tam, D. P. K. Tsang, M. Y. Chan, N. Y. Zhu, V. W. W. Yam, *Chem. Commun.* **2011**, *47*, 3383–3385; g) A. K. W. Chan, M. Ng, Y. C. Wong, M. Y. Chan, W. T. Wong, V. W. W. Yam, *J. Am. Chem. Soc.* **2017**, *139*, 10750–10761; h) E. Garoni, J. Boixel, V. Dorcet, T. Roisnel, D. Roberto, D. Jacquemin, V. Guerchais, *Dalton Trans.* **2018**, *47*, 224–232.
[12] a) M. Cocchi, J. Kalinowski, V. Fattori, J. A. G. Williams, L. Murphy, *Appl. Phys. Lett.* **2009**, *94*, 073309; b) W. Mróz, C. Botta, U. Giovanella, E. Rossi, A. Colombo, C. Dragonetti, D. Roberto, R. Ugo, A. Valore, J. A. G. Williams, *J. Mater. Chem.* **2011**, *21*, 8653–8661; c) E. Rossi, A. Colombo, C. Dragonetti, D. Roberto, R. Ugo, A. Valore, L. Falciola, P. Brulatti, M. Cocchi, J. A. G. Williams, *J. Mater. Chem.* **2012**, *22*, 10650–10655; d) L. Murphy, P. Brulatti, V. Fattori, M. Cocchi, J. A. G. Williams, *Chem. Commun.* **2012**, *48*, 5817–5819.
[13] a) S. W. Botchway, M. Charnley, J. W. Haycock, A. W. Parker, D. L. Rochester, J. A. Weinstein, J. A. G. Williams, *Proc. Nat. Acad. Sci, USA* **2008**, *105*, 16071–16076; b) E. Baggaley, S. W. Botchway, J. W. Haycock, H. Morris, I. V. Sazanovich, J. A. G. Williams, J. A. Weinstein, *Chem. Sci.* **2014**, *5*, 879–886; c) E. Baggaley, I. V. Sazanovich, J. A. G. Williams, J. W. Haycock, S. W. Botchway, J. A. Weinstein, *RSC Adv.* **2014**, *4*, 35003–35008.
[14] a) D. J. Cárdenas, A. M. Echavarren, M. C. Ramírez de Arellano, *Organometallics* **1999**, *18*, 3337–3341; b) J. A. G. Williams, *Chem. Soc. Rev.* **2009**, *38*, 1783–1801.
[15] a) L. Murphy, A. Congreve, L. O. Palsson, J. A. G. Williams, *Chem. Commun.* **2010**, *46*, 8743–8745; b) M. T. Walden, P. Pander, D. S. Yufit, F. B. Dias, J. A. G. Williams, *J. Mater. Chem. C* **2019**, *7*, 6592–6606.
[16] a) Y. Chi, B. Tong, P. T. Chou, *Coord. Chem. Rev.* **2014**, *281*, 1–25; b) S. Y. Chang, J. Kavitha, S. W. Li, C. S. Hsu, Y. Chi, Y. S. Yeh, P. T. Chou, G. H. Lee, A. J. Carty, Y. T. Tao, C. H. Chien, *Inorg. Chem.* **2006**, *45*, 137–146; c) S. Y. Chang, J. Kavitha, J. Y. Hung, Y. Chi, Y. M. Cheng, E. Y. Li, P. T. Chou, G. H. Lee, A. J. Carty, *Inorg. Chem.* **2007**, *46*, 7064–7074.
[17] a) K. Hanson, L. Roskop, P. I. Djurovich, F. Zahariev, M. S. Gordon, M. E. Thompson, *J. Am. Chem. Soc.* **2010**, *132*, 16247–16255; b) K. Hanson, L. Roskop, N. Patel, L. Griffe, P. I. Djurovich, M. S. Gordon, M. E. Thompson, *Dalton Trans.* **2012**, *41*, 8648–8659.
[18] a) H.-M. Wen, Y.-H. Wu, Y. Fan, L.-Y. Zhang, C.-N. Chen, Z.-N. Chen, *Inorg. Chem.* **2010**, *49*, 2210–2221; b) H.-M. Wen, Y.-H. Wu, L.-J. Xu, L.-Y. Zhang, C.-N. Chen, Z.-N. Chen, *Dalton Trans.* **2011**, ***40***, 6929–6938.
[19] a) P. Mandapati, J. D. Braun, C. Killeen, R. L. Davis, J. A. G. Williams, D. E. Herbert, *Inorg. Chem.* **2019**, *58*, 14808–14817; b) P. Mandapati, J. D. Braun, I. B. Lozada, J. A. G. Williams, D. E. Herbert, *Inorg. Chem.* **2020**, 59, 12504–12517.
[20] P. J. S. Miguel, M. Roitzsch, L. Yin, P. M. Lax, L. Holland, O. Krizanovic, M. Lutterbeck, M. Schürmann, E. C. Fusch, B. Lippert, *Dalton Trans.* **2009**, 10774–10786.
[21] E. I. Lerner, S. J. Lippard, *J. Am. Chem. Soc.* **1976**, *98*, 5397–5398.
[22] a) I. Castro, J. Sletten, J. Faus, M. Julve, Y. Journaux, F. Lloret, S. Alvarez, *Inorg. Chem.* **1992**, *31*, 1889–1894; b) P. Paul, B. Tyagi, M. M. Bhadbhade, E. Suresh, *J. Chem. Soc. Dalton Trans.* **1997**, 2273–2278; c) B. Vangdal, J. Carranza, F. Lloret, M. Julve, J. Sletten, *J. Chem. Soc. Dalton Trans.* **2002**, 566–574; d) A. Kamiyama, T. Noguchi, T. Kajiwara, T. Ito, *Inorg. Chem.* **2002**, *41*, 507–512; e) M. G. Cowan, S. Brooker, *Dalton Trans.* **2012**, *41*, 1465–1474.
[23] V. S. Arvapalli, G. Chen, S. Kosarev, M. E. Tan, D. Xie, Y. Let, *Tetrahedron Lett.* **2010**, *51*, 284–286.
[24] D. J. van Dijken, P. Kovaříček, S. P. Ihrig, S. Hecht, *J. Am. Chem. Soc.* **2015**, *137*, 14982–14991.
[25] F. Kitamura, K. Sawaguchi, A. Mori, S. Takagi, T. Suzuki, A. Kobayashi, M. Kato, K. Nakajima, *Inorg. Chem.* **2015**, *54*, 8436–8448.
[26] a) V. N. Kozhevnikov, M. C. Durrant, J. A. G. Williams, *Inorg. Chem.* **2011**, *50*, 6304–6313; b) S. Culham, P.-H. Lanoë, V. L. Whittle, M. C. Durrant, J. A. G. Williams, V. N. Kozhevnikov, *Inorg. Chem.* **2013**, *52*, 10992–11003; c) R. Muñoz-Rodriguez, E. Buñuel, N. Fuentes, J. A. G. Williams, D. J. Cárdenas, *Dalton Trans.* **2015**, *44*, 8394–8405; d) G. Turnbull, J. A. G. Williams, V. N. Kozhevnikov, *Chem. Commun.* **2017**, *53*, 2729–2732.
[27] A. Mori, T. Suzuki, Y. Nakatani, Y. Sunatsuki, M. Kojima, K. Nakajima, *Dalton Trans.* **2015**, *44*, 15757–15760.
[28] a) Q. Zhao, L. Li, F. Y. Li, M. X. Yu, Z. P. Liu, T. Yi, C. H. Huang, *Chem. Commun.* **2008**, 685–687; b) Y. You, H. S. Huh, K. S. Kim, S. W. Lee, D. Kim, S. Y. Park, *Chem. Commun.* **2008**, 3998–4000; c) K. Huang, H. Wu, M. Shi, F. Li, T. Yi, C. Huang, *Chem. Commun.* **2009**, 1243–1245; d) A. J. Howarth, R. Patia, D. L. Davies, F. Lelj, M. O. Wolf, K. Singh, *Eur. J. Inorg. Chem.* **2014**, 3657–3664.
[29] a) C.-F. Yan, L. Chen, R. Feng, M. Yang, F.-L. Jiang, M.-C. Hong, *Chinese J. Struc. Chem.* **2009**, *28*, 1099–1104; b) K. Ha, *Z. Kristallogr. NCS* **2010**, *225*, 789–790.
[30] See, for example, X. Zhang, S. Abid, L. Shi, J. A. G. Williams, M. A. Fox, F. Miomandre, C. Tourbillon, J.-F. Audibert, O. Mongin, F. Paul, C. O. Paul-Roth, *Dalton Trans.* **2019**, *48*, 11897–11911.
[31] a) S. Lamansky, P. Djurovich, D. Murphy, F. Abdel-Razzaq, H. E. Lee, C. Adachi, P. E. Burrows, S. R. Forrest, M. E. Thompson, *J. Am. Chem. Soc.* **2001**, *123*, 4304–4312; b) Y. Wang, P. Bao, J. Wang, R. Jia, F. Q. Bai, H. X. Zhang, *Inorg. Chem.* **2018**, *57*, 6561–6570.
[32] a) V. W. W. Yam, R. P. L. Tang, K. M. C. Wong, K. K. Cheung, *Organometallics* **2001**, *20*, 4476–4482; b) W. H. Lam, E. S. H. Lam, V. W. W. Yam, *J. Am. Chem. Soc.* **2013**, *135*, 15135–15143; c) K. L. Garner, L. F. Parkes, J. D. Piper, J. A. G. Williams, *Inorg. Chem.* **2010**, *49*, 476–487.
[33] P. K. Chow, C. S. Ma, W. P. To, G. S. M. Tong, S. L. Lai, S. C. F. Kui, W. M. Kwok, C. M. Che, *Angew. Chem. Int. Ed.* **2013**, *52*, 11775–11779; *Angew. Chem.* **2013**, *125*, 11991–11995.
[34] D. Drew, J. R. Doyle, *Inorg. Synth.* **1990**, *28*, 346–349.
[35] K. Suzuki, A. Kobayashi, S. Kaneko, K. Takehira, T. Yoshihara, H. Ishida, Y. Shiina, S. Oishi, S. Tobita, *Phys. Chem. Chem. Phys.* **2009**, *11*, 9850–9860.
[36] Gaussian 16, Revision C.01, M. J. Frisch, G. W. Trucks, H. B. Schlegel, G. E. Scuseria, M. A. Robb, J. R. Cheeseman, G. Scalmani, V. Barone, G. A. Petersson, H. Nakatsuji, X. Li, M. Caricato, A. V. Marenich, J. Bloino, B. G. Janesko, R. Gomperts, B. Mennucci, H. P. Hratchian, J. V. Ortiz, A. F. Izmaylov, J. L. Sonnenberg, D. Williams-Young, F. Ding, F. Lipparini, F. Egidi, J. Goings, B. Peng, A. Petrone, T. Henderson, D. Ranasinghe, V. G. Zakrzewski, J. Gao, N. Rega, G. Zheng, W. Liang, M. Hada, M. Ehara, K. Toyota, R. Fukuda, J. Hasegawa, M. Ishida, T. Nakajima, Y. Honda, O. Kitao, H. Nakai, T. Vreven, K. Throssell, J. A. Montgomery, Jr., J. E. Peralta, F. Ogliaro, M. J. Bearpark, J. J. Heyd, E. N. Brothers, K. N. Kudin, V. N. Staroverov, T. A. Keith, R. Kobayashi, J. Normand, K. Raghavachari, A. P. Rendell, J. C. Burant, S. S. Iyengar, J. Tomasi, M. Cossi, J. M. Millam, M. Klene, C. Adamo, R. Cammi, J. W. Ochterski, R. L. Martin, K. Morokuma, O. Farkas, J. B. Foresman, D. J. Fox, Gaussian, Inc., Wallingford CT, **2019**.
[37] T. Yanai, D. P. Tew, N. C. Handy, *Chem. Phys. Lett.* **2004**, *393*, 51–57.
[38] Dalton, a molecular electronic structure program, Release v2018.2 (2019), see http://daltonprogram.org.
[39] A. D. Boese, J. M. L. Martin, *J. Phys. Chem.* **2004**, *121*, 3405–3416.
[40] J.-D. Chai, M. Head-Gordon, *Phys. Chem. Chem. Phys.* **2008**, *10*, 6615–6620.

Manuscript received: September 18, 2020
Revised manuscript received: November 23, 2020